Research Article | Vol. 28, No. 25 / 7 December 2020 / Optics Express 38334

Optics EXPRESS

Measurement of the Kerr nonlinear refractive index of the Rb vapor based on an optical frequency comb using the z-scan method

SANDAN WANG,[1,2] JINPENG YUAN,[1,2,3] LIRONG WANG,[1,2,4] LIANTUAN XIAO,[1,2] AND SUOTANG JIA[1,2]

[1] State Key Laboratory of Quantum Optics and Quantum Optics Devices, Institute of Laser Spectroscopy, Shanxi University, 92 Wucheng Road, Taiyuan 030006, China
[2] Collaborative Innovation Center of Extreme Optics, Shanxi University, 92 Wucheng Road, Taiyuan 030006, China
[3] yjp@sxu.edu.cn
[4] wlr@sxu.edu.cn

Abstract: We report the measurement of the Kerr nonlinear refractive index of the rubidium vapor via the high sensitivity z-scan method by using an optical frequency comb. The novel self-focusing and self-defocusing effects of the vapor are presented with red and blue detunings of the laser frequency. The optical nonlinear characteristics of the rubidium vapor are clearly interpreted under different experimental parameters. Furthermore, the Kerr nonlinear refractive index n_2 is obtained from the measured dispersion curve, and it basically occurs on the order of 10^{-6} cm^2/W. The evolutions of the Kerr nonlinear coefficient n_2 with the laser power and frequency detuning, respectively, are studied. To the best of our knowledge, the use of pulsed lasers to measure the Kerr nonlinear refractive index n_2 of atomic vapor has not been reported yet. The direct measurement of the Kerr nonlinear coefficient will greatly help us understand and optimize nonlinear optical processes and find its more potential applications in quantum optics.

1. Introduction

The alkali atomic vapor has been used as a robust nonlinear material in the field of quantum optics [1–3]. The precision measurement of the Kerr nonlinear refractive index n_2 for atomic vapor through enhanced nonlinear optical processes is employed in many research fields. A completely controllable nonlinear optical system can be achieved by understanding the evolution of the Kerr nonlinear coefficient. The study of optical nonlinear characteristics has led to many valuable applications including all-optical switches [4,5], optical soliton generation [6], frequency conversion [7], quantum information processing [8,9], and laser frequency stabilization [10].

To measure nonlinear refractive index, several methods were employed including nonlinear interferometry [11], multi-wave mixing [12,13], ellipse rotation [14], and beam distortion measurements [15]. Interferometry and multi-wave mixing require multi-beam measurement, thereby increasing the complexity of the experimental system. Ellipse rotation is insensitive measurement and requires complicated wave-propagation analysis. The z-scan method, which is based on the spatial beam distortion principle, was proposed as a simple and easy-to-implement method for measuring the Kerr coefficient n_2 [16]. The single-beam optical configuration of z-scan is a convenient and compact integration component. The sign and magnitude of nonlinear absorption and refraction can be simultaneously measured to determine the properties of the measured nonlinear material. Importantly, the evolution of nonlinear optical characteristics can also be depicted owing to the dynamic measurement process.

The Kerr nonlinear refractive index n_2 of atomic vapor, as an important nonlinear parameter, can be used to control the relative contributions of linear and nonlinear effects in real-time

#413350 https://doi.org/10.1364/OE.413350
Journal © 2020 Received 26 Oct 2020; revised 20 Nov 2020; accepted 23 Nov 2020; published 3 Dec 2020

Optics EXPRESS

by adjusting the experimental parameters [17,18]. The self-induced absorptive and refractive nonlinear behaviors of the hot Na vapor [19], Rb vapor [20], Cs vapor [21], and a cloud of cold Cs atoms [22] were investigated by the z-scan method. Additionally, the Kerr coefficient for both red and blue detunings of the hot atomic rubidium vapor was measured [23]. A variant of the z-scan method was applied to measure the nonlinear refractive coefficients for the Cs vapor by scanning the laser frequency for different sample positions [24]. The use of pulse lasers to perform precision measurement has gained significant interest because of the development of phase-stabilized optical frequency combs (OFCs) [25]. Because of the high peak intensity of pulse lasers, the significant nonlinear effect of an atomic vapor can be observed at low average power [26]. Additionally, a stabilized OFC, which contains approximately 10^5-10^6 optical frequency components spanning the entire visible spectrum, can realize the multi-channel broadband measurements with high-sensitivity [27]. However, there is no reports on measuring the Kerr nonlinear refractive index n_2 of atomic vapor with pulsed lasers to the best of our knowledge. The OFC can be used as a femtosecond pulsed laser with stable frequency and finely tunable frequency detuning to obtain high nonlinear refractive index at extremely low average power.

In this study, we investigate the third-order nonlinear refractive index n_2 of the rubidium thin vapor with a stabilized OFC by using the z-scan method. Distinct self-defocusing and self-focusing dispersion curves of the vapor at red and blue detunings are obtained. The nonlinear refractive index n_2 is studied under different laser frequency detuning and average power. The dependence of the nonlinear characteristics of the rubidium vapor on systematic properties is also explored, which is essential for distinguishing between linear and nonlinear characteristic in atomic systems.

2. Experimental setup

The experimental implementation for measuring the Kerr nonlinear refractive index by using the z-scan method is shown in Fig. 1. The laser source used to excite the $5S_{1/2} - 5P_{3/2}$ transition of rubidium at 780 nm was provided by an OFC system (Menlo systems, FC1500), which covered a broadband wavelength range from 600 nm to 900 nm. The frequency of each optical mode can be expressed as $f_n = nf_{rep} + f_{ceo}$, where the repetition frequency f_{rep} is 250 MHz, and the offset frequency f_{ceo} is 20 MHz. The output of the OFC is filtered by using a tunable optical filter (TOF) with a full width at half maximum of 0.1 nm. The laser frequency detuning was achieved by precisely control of the repetition frequency of optical frequency comb. A Gaussian beam of diameter 2 mm from the OFC was collimated through a single-mode optical fiber (SMF). Subsequently, the collimated beam was focused by using a lens (L3) with a focal length of 20 cm to ensure that had a Rayleigh length of $z_R = 7$ mm and minimal waist of $\omega_0 = 40$ μm, which is checked all along the beam path using a beam quality analyzer. A thin rubidium vapor filled with pure ^{87}Rb, 22 mm in diameter and 1 mm in thickness, was placed behind the lens (L3) in the beam path. And a homemade temperature controller with fully enclosed copper configuration is employed to ensure a uniform atomic density. The vapor thickness was set significantly smaller than the Rayleigh length so that light propagation effects on the laser inside the vapor could be negligible. The temperature of the vapor is measured by a thermocouple thermometer and then accurately controlled to be 80 °C with the corresponding atomic density of $N = 1.55 \times 10^{18}$ m^{-3}. Additionally, the movement of the vapor cell was precisely controlled by using a linear translation stage (Thorlabs, LTS300), which had the minimum incremental movement of 0.1 μm and on-axis accuracy of 5 μm. Upon moving the vapor cell along the beam across the focal point, the laser intensity transmitted through the aperture (A) was modified because of the self-focusing or self-defocusing effects. Additionally, the aperture transmittance ratio S was 0.05. In the far field, the transmittance beam was detected by using a photodetector (PD).

Optics EXPRESS

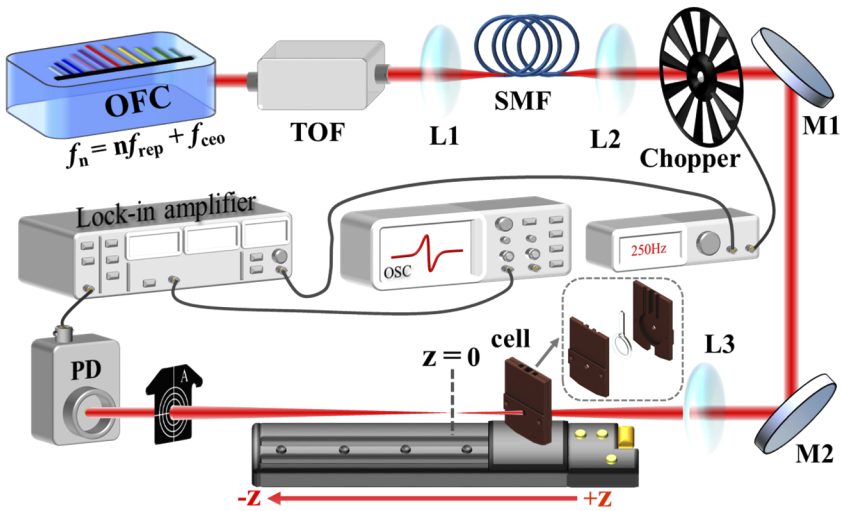

Fig. 1. Measuring the Kerr nonlinear refractive index by using the z-scan method. OFC: optical frequency comb system, f_{rep}: repetition frequency, f_{ceo}: offset frequency, TOF: tunable optical filter, L: lens, SMF: single-mode optical fiber, M: high reflection mirror, A: aperture, PD: photodetector, OSA: oscilloscope.

In the process of data acquisition, the power of the incident laser was kept fixed. The focal point of the lens was determined as the measurement zero point (z = 0), and the measured sample was moved along in the -z and +z directions of the linear translation stage. The laser power detected by the PD varied with the sample position, and this variation can be used to represent the normalized transmittance T(z) of the vapor at different sample positions. To perform a high sensitivity measurement, a robust intensity modulation method was employed. The laser intensity was modulated by using a chopper wheel (Stanford Research Systems, SR540) with an optimized modulation frequency of 250 Hz. The obtained signal of the PD was demodulated by using a lock-in amplifier (Stanford Research Systems, SR830).

3. Experimental results and discussions

The z-scan method used to measure the Kerr coefficient of a sample relies on the light propagation properties of a Gaussian beam along its transmission direction. The incident laser field can be expressed as follows [28]:

$$E(z,r,t) = E_0(t)\frac{\omega_0}{\omega(z)}exp(-\frac{r^2}{\omega(z)^2} - \frac{ikr^2}{2R(z)})exp(-i\varphi(z,t)) \tag{1}$$

where $E_0(t)$ denotes the field intensity at the focal point, $\omega(z) = \omega_0(1 + z^2/{z_0}^2)^{1/2}$ the spot size of the laser source at the z position, and $z_0 = k{\omega_0}^2/2$ the diffraction length of the laser. $R(z) = z(1 + {z_0}^2/z^2)$ is the expression for the curvature radius of the wave front at z, where $k = 2\pi/\lambda$ denotes the wave vector and φ the phase of the beam propagating in the medium. The intensity of the excited laser beam can be expressed as follows [28]:

$$I(z,r,t) = I_0(t)\frac{\omega_0^2}{\omega(z)^2}exp(-2\frac{r^2}{\omega(z)^2}) \tag{2}$$

If the thickness of the sample is less than the diffraction length, the phase change of the laser beam can be expressed as $\frac{\partial\varphi}{\partial z'} = kn_2I$, and the change in the laser intensity can be expressed as

Optics EXPRESS

$\frac{\partial I}{\partial z'} = -\alpha(I)I$. Therefore, $\Delta\varphi(z,r,t) = \frac{\Delta\varphi_0(t)}{1+\frac{z^2}{z_0{}^2}} exp(-\frac{2r^2}{\omega(t)^2})$, where $\Delta\varphi_0$ denotes the phase change amount of the laser beam at the focal point. Additionally, $\Delta\varphi_0$ can be represented by using the laser intensity I_0 at the focal point as follows [24,29]:

$$\Delta\varphi_0 = kn_2 I_0 L \tag{3}$$

where $k = \frac{2\pi}{\lambda}$, λ the light beam wavelength, L the cell thickness.

For a cell thickness significantly smaller than the beam Rayleigh length, the aperture transmittance as a function of the cell position z, relative to the focal point, is given as follows [24,29]:

$$T(x) = 1 - \frac{4\Delta\varphi_0 x}{(1+x^2)(9+x^2)} \tag{4}$$

where $x = z/z_R$, z the sample position relative to the focal point of the beam, and z_R the Rayleigh length. Thus, the Kerr nonlinear coefficient n_2 can be calculated by Eq. (3) using the $\Delta\varphi_0$ value obtained by fitting the dispersion curve with Eq. (4). In our experiment, when the laser frequency detuning is 0.7 GHz with the average power of 500 μW, the obtained maximum value of the $\Delta\varphi_0$ is 0.42, which is agreement with the relation of $\Delta\varphi_0 < \pi$.

Meanwhile, the standard equation for the Kerr coefficient of an atomic vapor can be derived by taking the limit of low intensity in a two-level atomic system since the Doppler width is much larger than the hyperfine interval of $5P_{3/2}$ state. For large detunings, n_2 can be expressed as follows [30,31] :

$$n_2(cm^2/W) = 10^4 \times \frac{\mu_{12}{}^4 N}{2c\varepsilon_0{}^2 h^3 \delta^3} \tag{5}$$

where μ_{12} denotes the dipole matrix element, N the number density of atoms, and $\delta = \nu - \nu_0$ the detuning from the resonance frequency. The linear dependence of the refractive index on $1/\delta^3$ makes n_2 antisymmetric in detuning.

For a thin media with positive nonlinear coefficients ($n_2 > 0$), the relative transmittance measured at the small aperture remains moderately consistent (T = 1) because of the weaker laser intensity upon moving from a position far away from the focal point (-z) to the focal point (z = 0). Upon scanning the sample near the focal point, the optical nonlinear refraction effect is significantly enhanced because of the increase in the laser intensity, making the far-field beam located at the small aperture divergent and decreasing the relative light transmittance (T < 1). If the sample continues to move from the focal point toward the +z direction, the self-focusing effect of the sample will cause the far-field beam to converge at the aperture, and the relative transmittance will increase (T > 1). In this situation, the thin medium exhibits a self-focusing effect. For thin media with negative nonlinear coefficients ($n_2 < 0$), the result is just the opposite and a self-defocusing effect is thus exhibited. Therefore, the sign and magnitude of n_2 can be obtained from the measured dispersion curve.

The dispersion curve of the vapor cell when the laser frequency is red detuning 0.7 GHz from $5S_{1/2} - 5P_{3/2}$ transition resonance is shown in Fig. 2(a). The curve shows an obvious feature of a pre-focal peak followed by a post-focal valley. The signal curves can be fitted using Eq. (4) to get $\Delta\varphi_0$, and then the Kerr coefficient n_2 can be calculated by using Eq. (3). The measured nonlinear refractive index n_2 is negative, meaning a clear self-defocusing effect. Contrarily, the curve demonstrated a pre-focal valley followed by a post-focal peak when the laser frequency is blue detuning of 0.9 GHz as shown in Fig. 2(b), indicating the positive nonlinear refractive index corresponding to the self-focusing effect.

Figure 3(a) and (b) shows dispersion curves with different average powers but opposite detunings, in which the power increased from 30 to 500 μW. Clearly, the dispersion intensity of the Rb vapor increases with increase in the laser power, meaning that $\Delta\varphi_0$ also gradually increases. Additionally, the linewidth of the dispersion curve is synchronously increase with the

Optics EXPRESS

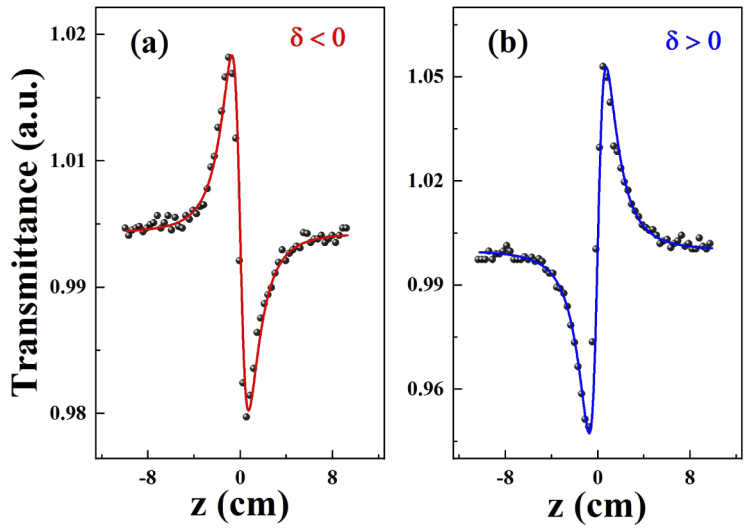

Fig. 2. Z-scan dispersion curve of the Rb vapor for: (a) red detuning δ = - 0.7 GHz with the self-defocusing effect and (b) blue detuning δ = 0.9 GHz with the self-focusing effect. The black dots represent the experimental data. The red and blue curves denote the fitting results of the experimental dots by using Eq. (4).

laser power because of the power broadening effect [32]. The laser frequency detuning directly affects the dispersion intensity of vapor as shown in Figs. 3(c) and 3(d). When the red laser frequency detuning was increased from 0.7 to 1.5 GHz, the dispersion intensity of the Rb vapor decreased. The case of blue laser frequency detuning showed a similar behavior. This similarity

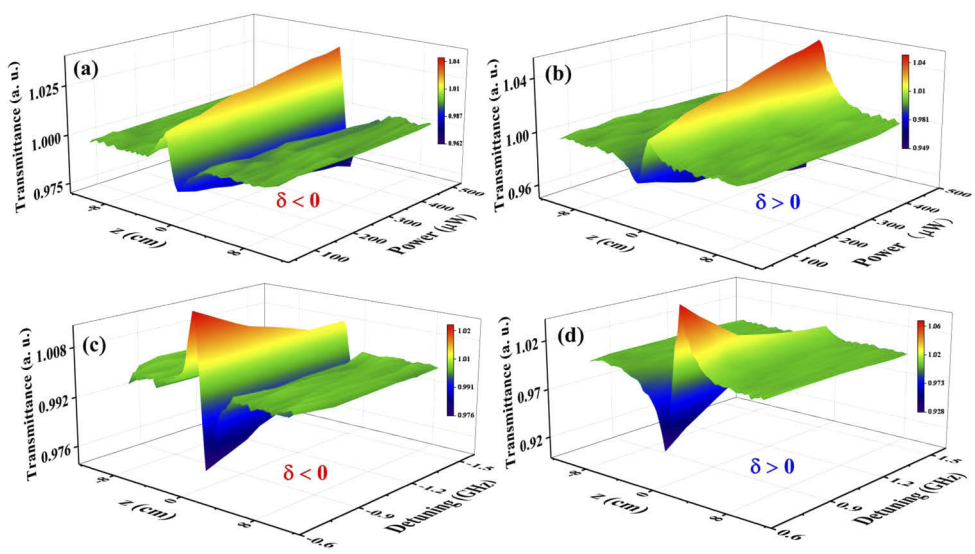

Fig. 3. Rubidium vapor dispersion curve versus the average power and frequency detuning of the laser. (a) and (b) depict the dispersion curves at different powers when δ = - 0.7 GHz and δ = 0.9 GHz, respectively. (c) and (d) depict the dispersion curves at different red and blue detunings when the laser average power is 300 μW.

Optics EXPRESS

is attributed to the dispersion effect of the atomic vapor becoming insignificant with increase in the frequency detuning [23].

The Kerr coefficient n_2 can be calculated from the obtained dispersion curve. Our measurement result $n_2 \approx 10^{-6}$ cm^2/W has an order of magnitude enhancement compared with the results obtained with continuous-wave lasers because of the high peak intensity of pulsed lasers, indicating that the nonlinearity of the rubidium vapor significantly increases. Compared with the third-order nonlinear refractive index, the fifth- and higher order nonlinear refractive index are small and can be neglected. Meanwhile, the same results can be obtained by using the technique of measuring the peak-to-valley amplitude of the dispersion curves (ΔT). Figures 4(a) and 4(b) show n_2 as a function of the average power for different laser frequency detunings of 0.7, 0.9, 1.1, 1.3, and 1.5 GHz, respectively. When the laser frequency is red detuning, n_2 is negative, indicating the self-defocusing effect. The absolute value of n_2 decreases as the laser power increases provided that the frequency detuning remains constant. The dependence between n_2 and laser power shows a clearly inversely proportional relationship, as can be seen from the theoretical fitting by Eq. (3). And the absolute value of n_2 remains constant when the power is higher than 500 μW. However, if the laser frequency is blue detuning, n_2 is positive corresponding to the self-focusing effect. Additionally, the trend of n_2 versus laser power is similar to that for the red detuning case.

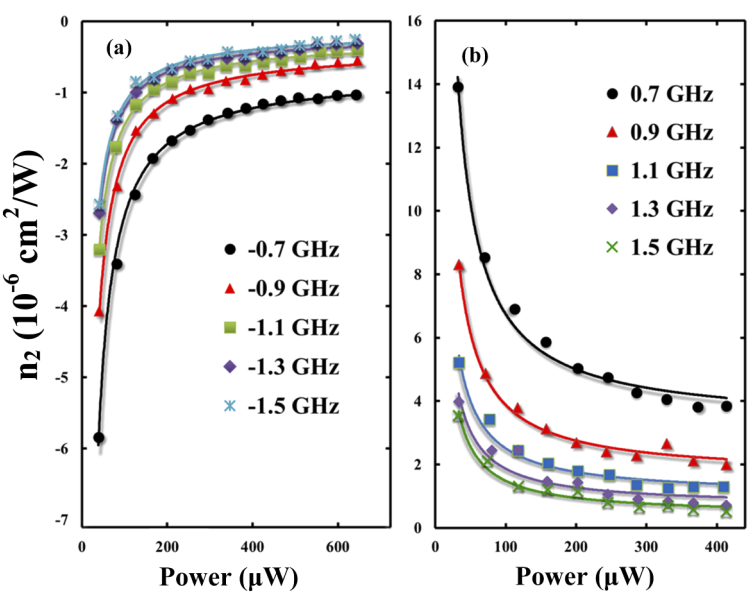

Fig. 4. Nonlinear Kerr coefficient n_2 as a function of the laser average power for different detunings. (a) Red detuning. (b) Blue detuning. The dots represent the experimental results and the lines refer to the theoretical fitting results.

Furthermore, the nonlinear Kerr coefficient n_2 is investigated as a function of the frequency detuning with different laser power (see Fig. 5). Clearly, the absolute value of n_2 decreases with increase in the frequency detuning, because the phase change amount $\Delta\varphi_0$ decreases as the laser detuning increases (see Figs. 3(c) and 3(d)). The experimental results and theoretical fitting results obtained by using Eq. (5) are in good agreement. Meanwhile, the cubic linear dependence between n_2 and frequency detuning is shown in the illustration of Fig. 5, which means the nonlinear effect of vapor can be greatly and conveniently enhanced by changing the frequency detuning. There are many interesting applications of the controllable nonlinearity of

Optics EXPRESS

the nonlinear refractive sign and magnitude by simply changing the frequency detuning, such as in all-optical switches and beam shaping.

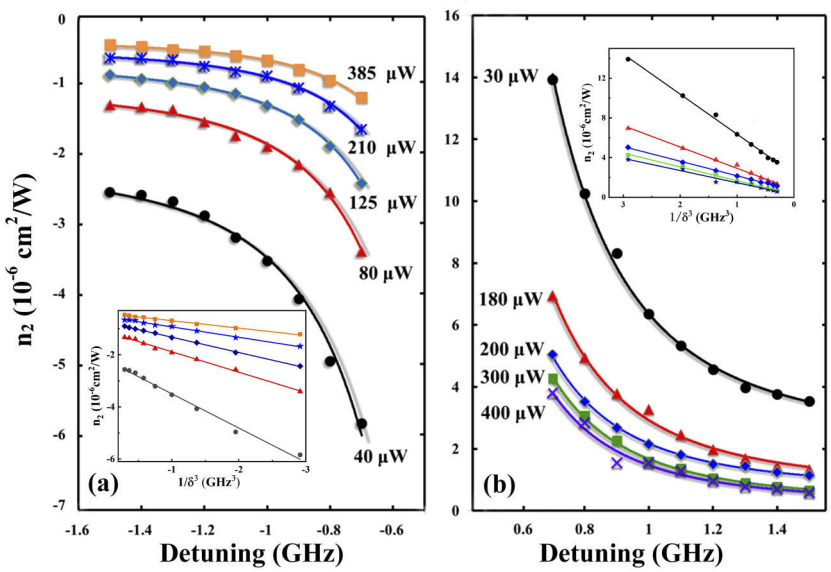

Fig. 5. Nonlinear refractive index n_2 versus the laser frequency detuning. (a) and (b) depict the case of red detuning and blue detuning, respectively. The dots represent the experimental results. The lines depict the theoretical fitting curves obtained by using Eq. (5). The insets represent the n_2 as a function of the cube of frequency detuning (δ^3).

4. Conclusions

In summary, we have experimentally demonstrated the optical nonlinearity of the rubidium vapor with an OFC by using the z-scan method. Self-defocusing and self-focusing effects were observed with red and blue frequency detunings. The Kerr nonlinear refractive index $n_2 \approx 10^{-6}$ cm^2/W, which is an order of magnitude enhancement compared with that in previous studies, was obtained from the dispersion curve. An inversely proportional relationship between the average power and n_2 was observed. Additionally, the dependence of n_2 on the cube of frequency detuning showed a clear linear relationship, and the experimental results agreed well with the theoretical fitting results. Such a precision measurement of the nonlinear coefficient n_2 would facilitate the understanding, optimization, and eventually complete control of the nonlinear optical processes in atomic systems. Additionally, our experimental research is of great significance to many quantum optics application including all-optical switches.

Funding

1331KSC; Key Research and Development Program of Shanxi Province for International Cooperation (201803D421034); Program for Sanjin Scholars of Shanxi Province; National Natural Science Foundation of China (61705122, 61875112, 62075121, 91736209); National Key Research and Development Program of China (2017YFA0304203).

Disclosures

The authors declare no conflicts of interest.

Optics EXPRESS

References

1. H. Cai, J. Liu, J. Wu, Y. He, S.-Y. Zhu, J.-X. Zhang, and D.-W. Wang, "Experimental observation of momentum-spacechiral edge currents in room-temperature atoms," Phys. Rev. Lett. **122**(2), 023601 (2019).
2. Z. Zhang, S. Liang, F. Li, S. Ning, Y. Li, G. Malpuech, Y. Zhang, M. Xiao, and D. Solnyshkov, "Spin-orbit coupling in photonic graphene," Optica **7**(5), 455–462 (2020).
3. Z. Zhang, R. Wang, Y. Zhang, Y. V. Kartashov, F. Li, H. Zhong, H. Guan, K. Gao, F. Li, Y. Zhang, and M. Xiao, "Observation of edge solitons in photonic graphene," Nat. Commun. **11**(1), 1902 (2020).
4. J. Sheng, U. Khadka, and M. Xiao, "Realization of all-optical multistate switching in an atomic coherent medium," Phys. Rev. Lett. **109**(22), 223906 (2012).
5. H. Wang, D. Goorskey, and M. Xiao, "Enhanced Kerr nonlinearity via atomic coherence in a three-level atomic system," Phys. Rev. Lett. **87**(7), 073601 (2001).
6. D. Xu, Z. Chen, and G. Huang, "Ultraslow weak-light solitons and their storage and retrieval in a kagome-structured hollow-core photonic crystal fiber," Opt. Express **25**(16), 19094–19111 (2017).
7. U. Khadka, J. Sheng, and M. Xiao, "Spatial domain interactions between ultraweak optical beams," Phys. Rev. Lett. **111**(22), 223601 (2013).
8. J. Yuan, C. Wu, L. Wang, G. Chen, and S. Jia, "Observation of diffraction pattern in two-dimensional optically induced atomic lattice," Opt. Lett. **44**(17), 4123–4126 (2019).
9. J. Yuan, S. Dong, C. Wu, L. Wang, L. Xiao, and S. Jia, "Optically tunable grating in a V + Ξ configuration involving a Rydberg state," Opt. Express **28**(16), 23820–23828 (2020).
10. W. Soares Martins, H. L. D. de S. Cavalcante, T. Passerat de Silans, M. Oriá, and M. Chevrollier, "Two-beam nonlinear Kerr effect to stabilize laser frequency with sub-Doppler resolution," Appl. Opt. **51**(21), 5080–5084 (2012).
11. J. Chandezon, J.-M. Rampnoux, S. Dilhaire, B. Audoin, and Y. Guillet, "In-line femtosecond common-path interferometer in reflection mode," Opt. Express **23**(21), 27011–27019 (2015).
12. Y. Kitagawa, R. L. Savage, and C. Joshi, "Demonstration of collisionally enhanced degenerate four-wave mixing in a plasma," Phys. Rev. Lett. **62**(2), 151–154 (1989).
13. J. J. Pigeon, S. Ya. Tochitsky, E. C. Welch, and C. Joshi, "Measurements of the nonlinear refractive index of air, N_2, and O_2 at 10 μm using four-wave mixing," Opt. Lett. **41**(17), 3924–3927 (2016).
14. J. A. C. Gomes, E. C. Barbano, and L. Misoguti, "Cross-section profile of the nonlinear refractive index of Gorilla Glass obtained by nonlinear ellipse rotation measurements," Appl. Opt. **58**(28), 7858–7861 (2019).
15. R. de Nalda, R. del Coso, J. Requejo-Isidro, J. Olivares, A. Suarez-Garcia, J. Solis, and C. N. Afonso, "Limits to the determination of the nonlinear refractive index by the z-scan method," J. Opt. Soc. Am. B **19**(2), 289–296 (2002).
16. M. Sheik-bahae, A. A. Said, and E. W. Van Stryland, "High-sensitivity, single-beam n_2 measurements," Opt. Lett. **14**(17), 955–957 (1989).
17. K.-J. Boller, A. Imamoglu, and S. E. Harris, "Observation of electromagnetically induced transparency," Phys. Rev. Lett. **66**(20), 2593–2596 (1991).
18. J. Yuan, C. Wu, Y. Li, L. Wang, Y. Zhang, L. Xiao, and S. Jia, "Integer and fractional electromagnetically induced Talbot effects in a ladder-type coherent atomic system," Opt. Express **27**(1), 92–101 (2019).
19. S. Sinha, G. K. Bhowmick, S. Kundu, S. Sasikumar, S. K. S. Nair, T. B. Pal, A. K. Ray, and K. Dasgupta, "A Z-scan study of nonlinear refraction in sodium vapour," Opt. Commun. **203**(3-6), 427–434 (2002).
20. C. F. McCormick, D. R. Solli, and R. Y. Chiao, "Nonlinear absorption and refraction in near-detuned rubidium vapor," J. Opt. Soc. Am. B **20**(12), 2480–2483 (2003).
21. M. O. Araujo, H. L. D. de S. Cavalcante, M. Oria, M. Chevrollier, and T. P. de Silans, "Measurement of the Kerr nonlinear refractive index of Cs vapor," Phys. Rev. A **88**(6), 063818 (2013).
22. Y. Wang and M. Saffman, "Experimental study of nonlinear focusing in a magneto-optical trap using a Z-scan technique," Phys. Rev. A **70**(1), 013801 (2004).
23. C. F. McCormick, D. R. Solli, and R. Y. Chiao, "Saturable nonlinear refraction in hot atomic vapor," Phys. Rev. A **69**(2), 023804 (2004).
24. F. C. Dias Dos Santos, J. C. De Aquino Carvalho, G. T. Moura, and T. Passreat De Silans, "Measurement of the nonlinear refractive index of Cs D1 line using z-scan," J. Opt. Soc. Am. B **36**(9), 2468–2472 (2019).
25. A. L. Gaeta, M. Lipson, and T. J. Kippenberg, "Photonic-chip-based frequency combs," Nat. Photonics **13**(3), 158–169 (2019).
26. C. B. Marble, J. E. Clary, G. D. Noojin, S. P. Oconnor, D. T. Nodurft, A. W. Wharmby, B. A. Rockwell, M. O. Scully, and V. V. Yakovlev, "Z-scan measurements of water from 1150 to 1400 nm," Opt. Lett. **43**(17), 4196–4199 (2018).
27. I. Barmes, S. Witte, and K. S. E. Eikema, "Spatial and spectral coherent control with frequency combs," Nat. Photonics **7**(1), 38–42 (2013).
28. Y. Jia, Z. F. Li, M. Saeed, J. Tang, H. Z. Cai, and Y. J. Xiang, "Kerr nonlinearity in germanium selenide nanoflakes measured by Z-scan and spatial self-phase modulation techniques and its applications in all-optical information conversion," Opt. Express **27**(15), 20857–20873 (2019).
29. M. Sheik-Bahae, A. A. Said, T.-H. Wei, D. J. Hagan, and E. W. V. Stryland, "Sensitive measurement of optical nonlinearities using a single beam," IEEE J. Quantum Electron. **26**(4), 760–769 (1990).
30. D. Grischkowsky, "Self-focusing of light by potassium vapor," Phys. Rev. Lett. **24**(16), 866–869 (1970).

Optics EXPRESS

31. D. Grischkowsky and J. A. Armstrong, "Self-defocusing of light by adiabatic following in rubidium vapor," Phys. Rev. A **6**(4), 1566–1570 (1972).
32. N. V. Vitanov, B. W. Shore, L. Yatsenko, K. Bohmer, T. Halfmann, T. Rickes, and K. Bergmann, "Power broadening revisited: theory and experiment," Opt. Commun. **199**(1-4), 117–126 (2001).